American Mineralogist, Volume 81, pages 327–334, 1996

High-pressure crystal chemistry of $LiScSiO_4$: An olivine with nearly isotropic compression

Robert M. Hazen, Robert T. Downs, and Larry W. Finger

Geophysical Laboratory and Center for High Pressure Research, Carnegie Institution of Washington, 5251 Broad Branch Road NW, Washington, DC 20015-1305, U.S.A.

Abstract

Single-crystal X-ray diffraction data have been obtained at several pressures to 5.6 GPa for synthetic $LiScSiO_4$ olivine. The bulk modulus is 118 ± 1 GPa, assuming $K' = 4$. This value is smaller than that of forsterite because compressibility of Li-O bonds in the M1 octahedral site is approximately twice that of the $M1^{2+}$-O bonds in other isomorphs. Compressibilities of *a, b,* and *c* orthorhombic axes are 2.70, 2.80, and 2.61 (all × 10^{-3} GPa^{-1}), respectively. This nearly isotropic compression (axial compression ratios = 1.00:1.04:0.97) contrasts with that of forsterite (1.00:1.99:1.55), fayalite (1.00:2.83:1.22), monticellite (1.00:1.85:1.10), and chrysoberyl (1.00:1.30:1.17). These differences arise from the distinctive distribution of cations of different valences and consequent differences in M1-O and M2-O bond compressibilities. The Li M1 octahedron displays a significant decrease in polyhedral distortions with pressure, a behavior not observed in other olivines.

Introduction

The high-pressure behavior of olivine has been studied extensively because of the important role of $(Mg,Fe)_2SiO_4$ in the Earth's upper mantle and transition zone (Ita and Stixrude 1992; Green 1994). Most experimental and theoretical studies have focused, therefore, on silicate olivines ($M_2^{2+}SiO_4$; M = Ni, Mg, Co, Fe, Mn, and Ca), which display extreme compressional anisotropy. The orthorhombic *b* axis in these compounds is approximately twice as compressible as *a,* a feature that results in seismic anisotropies in subducting slabs and other olivine-rich regions where crystals adopt a preferred orientation (see, for example, Russo and Silver 1995). High-pressure crystal structures of silicate olivines (Hazen 1976, 1977; Kudoh and Takeuchi 1985; Kudoh and Takeda 1986; Sharp et al. 1987) reveal that M1 and M2 octahedra with M^{2+}-O bonds are much more compressible than Si^{4+}-O bonds.

The behavior of $M_2^{2+}Si^{4+}O_4$ olivines contrasts with that of isostructural chrysoberyl $Al_2^{3+}Be^{2+}O_4$, which is more nearly isotropic in its compression. Hazen (1987) determined high-pressure crystal structures of chrysoberyl and ascribed its more uniform compression to the similar compressibilities of $^{[4]}Be^{2+}$ and $^{[6]}Al^{3+}$ units. The question remains, however, whether olivine is an intrinsically anisotropic structure or whether anisotropies arise from the mismatch of adjacent polyhedral units.

In both $M_2^{2+}SiO_4$ olivines and chrysoberyl, M1 and M2 octahedra are occupied by similar cations. It is not possible, therefore, to assess unambiguously the relative roles of these two octahedra in olivine's pressure response. The synthetic olivine $Li^{1+}Sc^{3+}Si^{4+}O_4$ (Ito 1977) provides an ideal isomorph for the study of the relative influence of M1 and M2 cations in olivine compression. The principal objective of this high-pressure structural study of $LiScSiO_4$ is to determine the relative compressibilities of M1, M2, and T polyhedra and thus to understand the contributions of these structural elements to the high-pressure behavior of olivine.

Experimental methods

Single crystals of synthetic $LiScSiO_4$ were obtained from the National Museum of Natural History, Smithsonian Institution (sample NMNH-136843). These crystals were synthesized by Ito (1977) using high-temperature (1250 °C) solvent growth techniques and slow cooling in air. Pure $LiScSiO_4$ samples were not available; the selected $LiScSiO_4$ sample was doped with approximately 0.5% Cr^{3+} substituting for Sc^{3+}. Pale green transparent crystals are euhedral, as described by Ito (1977), and up to 1 mm in length.

Room-pressure X-ray diffraction

Initial X-ray diffraction studies of crystals in air were conducted on a Rigaku AFC-5R single-crystal diffractometer operated at 45 kV and 180 mA. An equant crystal approximately 100 × 95 × 90 μm (hereafter crystal 0) was selected for preliminary examination. Orthorhombic lattice parameters (space group *Pbnm*), determined from positions of 25 reflections between 40 and 54° 2θ (Ralph and Finger 1982), are $a = 4.8168(9)$, $b = 10.4317(8)$, and $c = 5.9650(9)$ Å, and $V = 299.72(8)$ Å^3, as recorded in Table 1. These values are approximately 0.1% smaller than those reported by Steele et al. (1978) for pure $LiScSiO_4$ [$a = 4.821(1)$, $b = 10.444(1)$, $c = 5.973(1)$ Å, and $V = 300.8(1)$ Å^3]. The minor substitution

0003–004X/96/0304–0327$05.00

TABLE 1. $LiScSiO_4$ olivine cell parameters vs. pressure

P (GPa)	a (Å)	b (Å)	c (Å)	V (Å³)
		Crystal 0		
0.0*	4.8168(9)	10.4317(8)	5.9650(9)	299.72(8)
		Crystal 1		
0.0	4.8179(6)	10.4329(6)	5.9685(9)	300.00(6)
0.06*	4.8189(12)	10.4373(6)	5.9695(6)	300.25(8)
1.46*	4.7996(13)	10.3925(6)	5.9443(6)	296.51(8)
2.95*	4.7778(13)	10.3484(6)	5.9214(5)	292.77(8)
		Crystal 2		
3.02*	4.7802(9)	10.3514(6)	5.9224(5)	293.05(6)
3.36	4.7767(11)	10.3406(6)	5.9167(5)	292.25(7)
3.72*	4.7717(7)	10.3320(4)	5.9128(3)	291.51(5)
0.23*	4.8190(12)	10.4333(5)	5.9672(5)	300.02(8)
4.51*	4.7611(11)	10.3072(6)	5.9006(4)	289.56(7)
0.99*	4.8040(13)	10.4117(7)	5.9533(5)	297.77(8)
2.17*	4.7918(7)	10.3784(5)	5.9365(3)	295.22(4)
5.15*	4.7535(11)	10.2864(8)	5.8895(3)	287.98(6)
5.63**	4.7452(5)	10.2788(6)	5.8877(2)	287.17(4)
0.21*	4.8198(13)	10.4378(6)	5.9699(5)	300.34(8)

Note: Error in pressure is estimated to be 0.08 GPa. Equation of state (EOS) unconstrained: $V_0 = 300.17(5)$, $K_0 = 128(5)$ GPa, $K' = 0(2)$. EOS constrained: $V_0 = 300.16(6)$, $K_0 = 118(1)$ GPa, $K' = 4$.

* Intensity data were collected at these conditions.

** Unconstrained refinement, $\gamma = 89.94(1)°$.

TABLE 2. $LiScSiO_4$ olivine data collection and structure-refinement information

P (GPa)	Total no. $\|F\|$	Total no. $\|F\|$ obs.	R (int.) (%)	p*	R (obs.)	R_w (obs.)
0.00	479	389	2.7	0.000	0.027	0.014
0.06	230	222	3.2	0.048	0.059	0.061
0.21	221	193	4.3	0.027	0.043	0.051
0.23	222	184	3.7	0.020	0.036	0.046
0.99	224	187	3.9	0.018	0.034	0.050
1.46	235	228	4.2	0.050	0.062	0.064
2.17	216	186	4.0	0.025	0.041	0.063
3.02	216	201	3.8	0.038	0.055	0.061
3.72	212	186	5.4	0.035	0.055	0.066
4.51	206	173	4.3	0.025	0.042	0.054
5.15	210	174	3.6	0.027	0.041	0.045

* Weights were computed by $\sigma = \sqrt{\sigma_I^2 + p^2F^2}$, where σ_I is derived from counting statistics.

of 0.5% Cr^{3+} for Sc^{3+} in our sample is sufficient to explain these differences (Lumpkin and Ribbe 1983).

A hemisphere of intensity data was measured for this crystal to $(\sin\theta)/\lambda \leq 0.705$ Å^{-1} for Mo$K\alpha_1$ radiation ($\lambda = 0.7093$ Å). Crystal-structure refinements were performed with a modified version of program RFINE4 (Finger and Prince 1975) using neutral-atom scattering factors (Ibers and Hamilton 1974). All atoms were refined with anisotropic displacement parameters, and we included an isotropic extinction parameter (Becker and Coppens 1974) and occupancy parameters for M1 and M2, which contain Li and Sc, respectively. We find that the extinction parameter is zero within error, and that Li and Sc are fully ordered, as reported by Steele et al. (1978). Table 2 records refinement conditions for this and subsequent experiments, and refined parameters for $LiScSiO_4$ at room pressure are given in Table 3. All refined atomic coordinates (Table 3) and anisotropic displacement parameters of $LiScSiO_4$ at room pressure agree within one estimated standard deviation with those of Steele et al. (1978; see their Table 1). Our observed mean Si-O, Li-O, and Sc-O bond distances are 1.631, 2.184, and 2.118 Å, respectively (see Tables 4–6), in comparison with 1.633, 2.185, and 2.121 Å in the earlier study.

A second crystal approximately 80 × 60 × 40 μm (hereafter crystal 1), with a platelike habit appropriate for high-pressure X-ray study, was selected. Orthorhombic lattice parameters for this crystal, on the basis of 20 centered reflections between 18 and 42° 2θ, are $a = 4.8179(6)$, $b = 10.4329(6)$, $c = 5.9685(9)$ Å, and $V = 300.00(6)$ Å³.

High-pressure X-ray diffraction

Crystal 1 was mounted in a Merrill-Bassett diamond-anvil cell with 0.75 mm anvil faces, an Inconel 750X gasket with 0.35 mm hole, and a 4:1 methanol-ethanol hydrostatic pressure medium. Fragments of ruby < 10 μm maximum dimension provided an internal pressure calibrant, as described by Hazen and Finger (1982). X-ray position and intensity data were collected on a Huber automated four-circle diffractometer with monochromatized Mo$K\alpha$ radiation.

TABLE 3. $LiScSiO_4$ olivine structural parameters vs. pressure

P	Si			Sc			Li	O1		
(GPa)	x	y	B_{eq} (Å²)	x	y	B_{eq} (Å²)	B_{eq} (Å²)	x	y	B_{eq} (Å²)
0.0	0.4311(2)	0.09111(7)	0.43	0.9923(1)	0.27433(5)	0.42	1.45	0.7631(4)	0.1013(2)	0.62
0.06	0.4316(7)	0.0910(2)	0.44(5)	0.9926(5)	0.2744(1)	0.38(4)	1.6(3)	0.7646(20)	0.1010(5)	0.57(9)
0.21	0.4317(7)	0.0912(2)	0.38(4)	0.9923(5)	0.2743(1)	0.42(4)	1.6(3)	0.7655(17)	0.1007(5)	0.51(9)
0.23	0.4321(7)	0.0910(2)	0.48(4)	0.9917(5)	0.2746(1)	0.37(3)	1.3(2)	0.7628(17)	0.1002(5)	0.62(10)
0.99	0.4314(7)	0.0902(2)	0.47(4)	0.9908(5)	0.2742(1)	0.42(3)	1.6(2)	0.7638(17)	0.0992(5)	0.68(10)
1.46	0.4301(7)	0.0903(2)	0.38(5)	0.9914(5)	0.2742(1)	0.31(5)	2.0(3)	0.7629(21)	0.0997(5)	0.64(10)
2.17	0.4307(7)	0.0903(2)	0.46(4)	0.9906(5)	0.2739(1)	0.38(4)	1.3(3)	0.7619(18)	0.0996(5)	0.54(10)
3.02	0.4295(7)	0.0895(2)	0.38(5)	0.9898(5)	0.2739(2)	0.32(4)	1.2(3)	0.7585(20)	0.0986(5)	0.43(11)
3.72	0.4294(10)	0.0893(3)	0.46(6)	0.9894(7)	0.2739(2)	0.37(5)	1.2(3)	0.7634(25)	0.0987(7)	0.57(14)
4.51	0.4281(9)	0.0885(3)	0.39(4)	0.9876(7)	0.2736(2)	0.35(4)	1.1(3)	0.7620(23)	0.0977(6)	0.55(12)
5.15	0.4266(7)	0.0893(2)	0.36(4)	0.9868(5)	0.2735(1)	0.32(4)	1.2(3)	0.7587(18)	0.0968(5)	0.49(10)

Note: $z = 0.25$ for Si, Sc, O1, O2; $x = y = z = 0$ for Li; space group: *Pbnm*.

Crystal 1 was studied at three pressures in the sequence 0.06, 1.46, and 2.95 GPa. Pressures were calibrated before and after each set of diffraction experiments; these measurements agreed within ±0.08 GPa. Unit-cell parameters were determined from the centered positions of 17–20 reflections, as recorded in Table 1. At each pressure, intensities of all accessible reflections to $(\sin\theta)/\lambda \leq 0.705$ Å^{-1} were measured using step scans of ±0.5° on ω, a step size of 0.025°, and an effective scan rate of 0.25°/min. We used the Lehmann and Larsen (1974) algorithm to calculate integrated intensities and converted to structure factors, including a correction for crystal absorption. We obtained average structure factors by averaging symmetry equivalent reflections in Laue group *mmm*. At the first two pressures the internal agreement of symmetrically equivalent reflections was approximately 4%, a value typical of a well-centered crystal in a Merrill-Bassett cell. At the last pressure (2.95 GPa), however, the internal agreement increased to 6% as a result of gasket deformation and partial shielding of the crystal. The latter data were not processed further.

Another crystal approximately 110 × 65 × 45 μm (hereafter crystal 2) was mounted in the diamond-anvil cell with a slightly larger (0.40 mm) gasket hole than was used for crystal 1. Unit-cell parameters were obtained at pressures in the following order: 3.02, 3.36, 3.72, 0.23, 4.51, 0.99, 2.17, 5.15, 5.63, and 0.21 GPa. In addition, intensity data were collected at all pressures except 3.36 and 5.63 GPa. At 5.63 GPa, the highest pressure attained in these experiments, peaks broadened significantly, suggesting deviatoric stress–induced strain. At all lower pressures unconstrained (i.e., triclinic) refinement of unit-cell parameters yielded results that agreed within error with orthorhombic constrained cell parameters. At 5.63 GPa, however, the unconstrained γ angle is 89.94(1)°, a significant deviation from 90° that also points to crystal strain.

High-pressure intensity data were corrected for crystal and diamond-cell absorption effects and were averaged as described above. For each of the ten high-pressure data sets (two for crystal 1 and eight for crystal 2), the 11 variable positional parameters and six isotropic displacement parameters were refined as described above. Conditions of refinement are recorded in Table 2, and refined parameters are listed in Table 3. Calculated and observed structure factors for these refinements are available from the authors.

Results

Axial compressibilities and *P-V* equation of state

Unit-cell parameters at 12 pressures, including crystal 1 at three pressures and crystal 2 at nine pressures (Table 1), were used to determine the *P-V* equation of state. Axial compressibilities may be represented as linear functions of pressure (in gigapascals) on the basis of linear regression of pressure–cell-edge data, as recorded in Figure 1. No significant curvature was observed for any of the axes. Axial compressibilities are 0.00270, 0.00280, and 0.00261 GPa^{-1} for *a*, *b*, and *c* axes, respectively. Axial compression ratios, *a*:*b*:*c* = 1:1.04:0.97, are close to isotropic.

Data for 12 *P-V* experiments, fitted by the Levenberg-Marquardt method (Press et al. 1986) with weights on both pressure and volume and using a second-order Birch-Murnaghan equation of state ($K' = 4$), yield $V_0 = 300.16 \pm 0.06$ Å^3 and $K_0 = 118 \pm 1$ GPa. These data may also be fitted by using a third-order Birch-Murnaghan equation of state ($V_0 = 300.17 \pm 0.05$ Å^3, $K_0 = 128 \pm 4$ GPa, and $K' = 0 \pm 2$), though the total volume compression of about 4% at the highest pressure is not sufficient to provide a meaningful curvature (K').

High-pressure crystal structures

Selected bond distances, bond angles, and polyhedral parameters for $LiScSiO_4$ at room pressure and ten high pressures are listed in Tables 4–7. Li-O bonds in M1 display the greatest compression, shortening by approximately 2.5% (from 2.18 to 2.13 Å) between room pressure and 5.1 GPa. The M1 octahedral volume decreases from 13.2 to 12.3 Å^3, or >7% over this range. Sc-O bonds in M2, in contrast, shorten by approximately 0.7% (from 2.118 to 2.103 Å) for a polyhedral compression of 2%. Tetrahedral Si-O bonds are even less compressible than M2, exhibiting a small but significant shortening from 1.631 at room pressure to about 1.625 at the highest pres-

Table 3.—*Continued*

P	O2			O3			
(GPa)	*x*	*y*	B_{eq} (Å^2)	*x*	*y*	*z*	B_{eq} (Å^2)
0.0	0.1954(4)	0.4477(2)	0.63	0.2821(3)	0.1684(1)	0.0401(2)	0.62
0.06	0.1966(20)	0.4479(5)	0.57(10)	0.2845(13)	0.1679(3)	0.0399(7)	0.48(7)
0.21	0.1990(19)	0.4471(4)	0.64(9)	0.2844(11)	0.1680(3)	0.0399(6)	0.54(7)
0.23	0.2002(17)	0.4477(4)	0.48(9)	0.2827(10)	0.1684(3)	0.0392(6)	0.44(6)
0.99	0.1975(18)	0.4471(5)	0.58(9)	0.2821(11)	0.1684(3)	0.0393(6)	0.67(7)
1.46	0.1986(20)	0.4465(4)	0.34(10)	0.2822(12)	0.1673(3)	0.0398(7)	0.38(7)
2.17	0.2019(18)	0.4462(5)	0.47(10)	0.2804(11)	0.1673(3)	0.0384(7)	0.53(7)
3.02	0.2014(21)	0.4459(5)	0.41(11)	0.2763(13)	0.1673(4)	0.0390(7)	0.37(8)
3.72	0.2065(25)	0.4444(6)	0.51(13)	0.2790(16)	0.1664(4)	0.0389(9)	0.50(9)
4.51	0.2060(25)	0.4450(6)	0.74(13)	0.2759(14)	0.1670(4)	0.0382(8)	0.47(8)
5.15	0.2073(20)	0.4445(5)	0.57(10)	0.2748(13)	0.1667(4)	0.0382(7)	0.46(7)

TABLE 4. SiO_4 tetrahedral distances, angles, and distortion parameters vs. pressure for $LiScSiO_4$

P (GPa)	Si-O1	Si-O2	Si-O3	⟨Si-O⟩	*V*	Q.E.
0	1.603(2)	1.615(2)	1.654(1)	1.631	2.195	1.0100
0.06	1.608(10)	1.617(6)	1.649(5)	1.631	2.1944	1.0095
0.21	1.612(9)	1.631(6)	1.649(5)	1.635	2.2121	1.0098
0.23	1.596(8)	1.625(6)	1.659(5)	1.635	2.2086	1.0105
0.99	1.599(8)	1.614(6)	1.658(5)	1.632	2.1992	1.0103
1.46	1.600(10)	1.617(6)	1.645(5)	1.627	2.1776	1.0097
2.17	1.590(9)	1.625(6)	1.654(5)	1.631	2.1920	1.0104
3.02	1.575(10)	1.613(6)	1.657(5)	1.626	2.1682	1.0115
3.72	1.597(12)	1.631(8)	1.646(6)	1.630	2.1857	1.0111
4.51	1.593(11)	1.611(8)	1.656(6)	1.629	2.1807	1.0116
5.15	1.581(9)	1.610(7)	1.651(5)	1.624	2.1606	1.0113
Int.	1.604(4)	1.621(4)	1.653(2)	1.633(1)	2.202(5)	1.00985(18)
Slope	−0.0042(13)	−0.0012(13)	−0.0001(9)	−0.0014(4)	−0.0067(17)	0.00035(7)

Note: Distances in angstroms, volume in cubic angstroms, angles in degrees, and angular variance in degrees squared.

TABLE 5. LiO_6 (M1) octahedral distances, angles, and distortion parameters vs. pressure for $LiScSiO_4$ olivine

P (GPa)	Li-O1	Li-O2	Li-O3	⟨Li-O⟩	*V*	Q.E.	O1-Li-O2	O1-Li-O3	O2-Li-O3	O.A.V.
0	2.155(1)	2.162(1)	2.234(1)	2.184	13.145	1.0373	89.68(5)	82.09(6)	73.25(6)	124.9
0.06	2.150(6)	2.159(7)	2.238(5)	2.182	13.119	1.0375	89.9(2)	82.3(2)	73.1(2)	125.9
0.21	2.147(5)	2.153(6)	2.239(4)	2.180	13.094	1.0363	90.1(2)	82.2(2)	73.4(2)	121.9
0.23	2.151(5)	2.147(6)	2.235(4)	2.178	13.0735	1.0354	90.1(2)	82.5(2)	73.6(2)	118.9
0.99	2.138(5)	2.152(6)	2.228(4)	2.173	12.9895	1.0351	90.0(2)	82.5(2)	73.6(2)	118.0
1.46	2.139(6)	2.147(6)	2.217(4)	2.168	12.9028	1.0350	89.8(2)	82.6(2)	73.6(2)	117.9
2.17	2.138(5)	2.134(6)	2.208(4)	2.160	12.8063	1.0328	90.0(2)	82.7(2)	74.1(2)	111.0
3.02	2.137(6)	2.131(7)	2.190(5)	2.153	12.6971	1.0318	89.7(2)	82.8(2)	74.4(2)	107.7
3.72	2.121(7)	2.116(8)	2.186(6)	2.141	12.5138	1.0305	90.2(3)	82.7(3)	74.8(3)	104.0
4.51	2.115(7)	2.111(8)	2.177(5)	2.135	12.4111	1.0298	90.3(3)	82.8(3)	74.9(3)	101.7
5.15	2.115(5)	2.105(6)	2.167(5)	2.129	12.3399	1.0284	90.0(2)	83.2(2)	75.1(2)	97.0
Int.	2.151(2)	2.158(2)	2.238(1)	2.1824(7)	13.133(9)	1.0368(2)	89.89(8)	82.28(6)	73.25(6)	123.6(8)
Slope	−0.0071(7)	−0.0104(7)	−0.0140(5)	−0.0105(2)	−0.156(4)	−0.00164(9)	0.04(3)	0.15(2)	0.37(2)	−5.1(3)

Note: Distances in angstroms, volume in cubic angstroms, angles in degrees, and angular variance in degrees squared.

TABLE 6. ScO_6 (M2) octahedral distances, angles, and distortion parameters vs. pressure for $LiScSiO_4$ olivine

P (GPa)	Sc-O1	Sc-O2	Sc-O3	Sc-O3	⟨Sc-O⟩	*V*	Q.E.	O1-Sc-O2
0	2.116(2)	2.057(2)	2.177(1)	2.092(1)	2.1181	12.1754	1.0274	176.96(8)
0.06	2.118(7)	2.060(7)	2.188(5)	2.089(4)	2.1220	12.2304	1.0281	177.2(3)
0.21	2.116(7)	2.061(6)	2.188(5)	2.088(4)	2.1215	12.2273	1.0279	177.8(3)
0.23	2.128(7)	2.067(6)	2.186(4)	2.085(4)	2.1227	12.2607	1.0271	177.9(3)
0.99	2.124(6)	2.056(6)	2.178(5)	2.081(4)	2.1163	12.1466	1.0273	178.0(3)
1.46	2.120(7)	2.049(6)	2.177(5)	2.085(4)	2.1155	12.1313	1.0274	177.9(3)
2.17	2.116(7)	2.055(6)	2.175(5)	2.078(5)	2.1126	12.1075	1.0259	178.3(3)
3.02	2.125(7)	2.048(7)	2.158(5)	2.084(5)	2.1092	12.0603	1.0252	178.3(4)
3.72	2.108(9)	2.043(9)	2.169(6)	2.075(6)	2.1064	11.9989	1.0260	179.7(5)
4.51	2.107(8)	2.050(8)	2.157(5)	2.069(5)	2.1016	11.9359	1.0249	179.8(5)
5.15	2.116(7)	2.048(7)	2.154(5)	2.068(5)	2.1011	11.9327	1.0246	180.0(2)
Int.	2.121(3)	2.060(2)	2.185(2)	2.089(1)	2.1214(7)	12.23(1)	1.0277(2)	177.3(2)
Slope	−0.002(1)	−0.0030(8)	−0.0061(9)	−0.0039(5)	−0.0041(3)	−0.060(5)	−0.00062(8)	0.52(6)

Note: Distances in angstroms, volume in cubic angstroms, angles in degrees, and angular variance in degrees squared.

TABLE 4.—*Continued*

P (GPa)	O1-Si-O2	O1-Si-O3	O2-Si-O3	O3-Si-O3	T.A.V.
0	115.97(11)	113.63(7)	106.74(7)	98.46(10)	42.6
0.06	116.2(4)	113.4(2)	106.6(3)	99.0(4)	40.2
0.21	116.3(4)	113.5(2)	106.4(3)	99.0(3)	41.5
0.23	116.6(3)	113.8(2)	106.1(3)	98.6(3)	45.9
0.99	115.9(4)	113.8(2)	106.7(3)	98.3(3)	43.9
1.46	116.0(4)	113.6(2)	106.6(3)	98.8(3)	41.5
2.17	116.5(4)	113.9(2)	105.9(3)	98.9(3)	45.3
3.02	116.3(4)	114.3(3)	106.0(3)	97.9(4)	50.3
3.72	116.9(5)	114.0(3)	105.7(4)	98.7(5)	48.0
4.51	116.8(5)	114.1(3)	106.0(3)	98.0(4)	50.3
5.15	116.5(4)	114.2(3)	106.0(3)	98.1(4)	49.2
Int.	116.13(12)	113.61(8)	106.52(12)	98.78(15)	42.1(9)
Slope	0.11(5)	0.12(3)	−0.14(4)	−0.13(6)	1.7(4)

sures, for a 0.4% change, and a corresponding volume compression of about 1%. Compressibilities of M1, M2, and T are thus 0.0119, 0.0049, and 0.0032 GPa^{-1} (polyhedral bulk moduli are 84, 204, and 315 GPa), respectively. Comparison of these values with predicted compressibilities of 0.0139, 0.0042, and 0.0015, based on bulk modulus-volume systematics, reveals that polyhedral compressibilities are proportional to polyhedral volume and inversely proportional to cation valence (Hazen and Finger 1979, 1982).

Polyhedral distortion, as measured by quadratic elongation and angle variance (Robinson et al. 1971), does not change significantly for the Si tetrahedron or the Sc (M2) octahedron (see Tables 4 and 6). The Li (M1) octahedron, however, becomes significantly more regular at higher pressure (Table 5): Quadratic elongation decreases from 1.037 to 1.028, and angle variance decreases from 125 to approximately 100. Quadratic elongation decreases because the longest Li-O bonds (Li-O3) are significantly more compressible than Li-O2 or Li-O1 bonds, as illustrated in Figure 2. Similarly, M1 angle variance decreases because O2-Li-O3 angles, which deviate the most from 90°, become closer to that ideal value with increasing pressure.

The relative orientations of M1, M2, and T are constrained by edge sharing among these polyhedra. Consequently, cation-anion-cation angles do not generally change significantly with pressure. The T-O2-M2 angle is an exception, however: Between room pressure and 5.15 GPa it decreases from 129.4 to 125.9° (see Table 7).

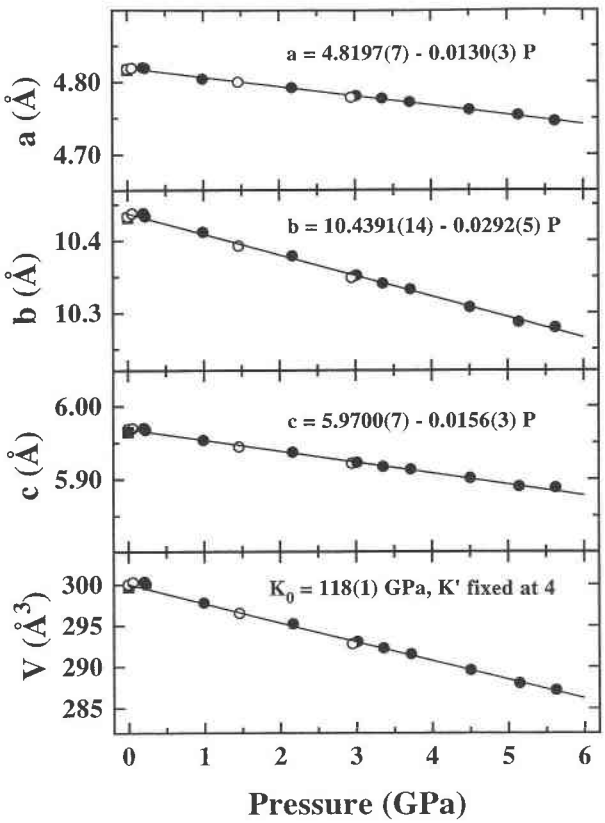

FIGURE 1. Orthorhombic unit-cell parameters for $LiScSiO_4$ as a function of pressure. Data for crystal 0 are identified with a square, crystal 1 with open circles, and crystal 2 with solid circles. Data at 2.95 and 5.63 GPa were not included in regression analysis (see text).

DISCUSSION

Olivine polyhedral bulk moduli and compressional anisotropy

The most surprising feature of the high-pressure behavior of $LiScSiO_4$ is the absence of compressional an-

TABLE 6.—*Continued*

P (GPa)	O1-Sc-O3	O1-Sc-O3	O2-Sc-O3	O2-Sc-O3	O3-Sc-O3	O3-Sc-O3	O3-Sc-O3	O3-Sc-O3	O.A.V.
0	84.36(6)	89.48(5)	98.12(5)	88.81(5)	88.82(3)	158.63(6)	70.25(7)	111.63(7)	96.3
0.06	84.2(2)	89.9(2)	98.0(2)	88.6(2)	88.87(8)	158.4(2)	69.9(2)	111.9(3)	98.5
0.21	84.2(2)	90.0(2)	97.6(2)	88.8(2)	88.85(9)	158.4(2)	70.0(2)	111.9(3)	97.5
0.23	84.2(2)	89.6(2)	97.5(2)	89.2(2)	88.76(9)	158.6(2)	70.3(2)	111.7(3)	95.1
0.99	84.0(2)	90.0(2)	97.6(2)	88.9(2)	88.75(9)	158.7(2)	70.3(2)	111.8(3)	95.8
1.46	84.0(2)	90.0(2)	97.7(2)	88.8(2)	89.04(8)	158.7(2)	70.0(2)	111.5(3)	96.0
2.17	84.0(2)	90.0(2)	97.4(2)	89.1(2)	89.02(9)	159.2(2)	70.6(2)	111.0(3)	91.1
3.02	83.9(2)	89.7(2)	97.5(3)	89.3(2)	89.1(1)	159.4(2)	70.8(3)	110.5(3)	89.1
3.72	83.4(3)	90.4(3)	96.8(3)	89.4(2)	89.2(1)	159.1(3)	70.3(3)	110.8(4)	91.2
4.51	83.5(3)	90.4(2)	96.7(3)	89.6(2)	89.1(1)	159.5(2)	70.8(3)	110.5(3)	87.8
5.15	83.5(2)	90.3(2)	96.5(2)	89.6(2)	89.2(1)	159.6(2)	70.8(3)	110.3(3)	86.6
Int.	84.25(5)	89.73(9)	97.92(10)	88.77(7)	88.82(4)	158.51(6)	70.09(9)	111.83(9)	97.3(6)
Slope	−0.16(2)	0.12(3)	−0.26(4)	0.17(3)	0.08(1)	0.22(2)	0.14(3)	−0.31(3)	−2.1(2)

TABLE 7. $LiScSiO_4$ olivine interpolyhedral angles vs. pressure

P (GPa)	Si-O1-Li	Si-O1-Sc	Li-O1-Li	Li-O1-Sc	Si-O2-Li	Si-O2-Sc	Li-O2-Li
0	119.73(7)	125.24(12)	87.60(7)	98.17(7)	91.30(7)	129.42(11)	87.23(7)
0.06	119.7(3)	125.0(4)	87.9(3)	98.4(3)	91.5(2)	129.1(6)	87.5(4)
0.21	119.7(2)	124.6(3)	88.1(3)	98.5(3)	91.4(2)	128.4(5)	87.7(3)
0.23	120.1(2)	124.7(3)	87.9(3)	98.1(3)	91.7(2)	127.8(5)	88.0(3)
0.99	120.1(2)	124.3(3)	88.3(3)	98.2(3)	91.3(2)	128.6(5)	87.5(3)
1.46	120.1(3)	124.7(4)	88.0(3)	98.0(3)	91.1(2)	128.5(5)	87.6(3)
2.17	120.2(3)	124.7(3)	87.9(3)	97.9(3)	91.2(2)	127.5(5)	88.1(3)
3.02	120.7(3)	124.8(4)	87.7(3)	97.3(3)	91.0(2)	127.6(6)	88.0(3)
3.72	120.2(3)	124.3(5)	88.4(4)	98.1(4)	90.8(3)	126.1(7)	88.6(4)
4.51	120.4(3)	124.1(4)	88.4(4)	97.9(4)	90.9(3)	126.2(7)	88.7(4)
5.15	121.0(3)	124.0(4)	88.2(3)	97.3(3)	90.7(2)	125.9(6)	88.8(3)
Int.	119.8(1)	124.9(1)	87.9(1)	98.3(1)	91.45(7)	128.9(2)	87.5(1)
Slope	0.19(4)	−0.16(4)	0.08(4)	−0.15(5)	−0.14(3)	−0.59(8)	0.25(4)

Note: Angles in degrees.

isotropy (axial ratios $a:b:c$ = 1.00:1.04:0.97). Anisotropy is pronounced in natural olivines, including forsterite (1.00:1.99:1.55; Hazen 1976; Hazen and Finger 1980; Kudoh and Takeuchi 1985; Downs et al. 1996), fayalite (1.00:2.83:1.22; Hazen 1977; Kudoh and Takeda 1986), monticellite (1.00:1.85:1.10; Sharp et al. 1987), and chrysoberyl (1.00:1.30:1.17; Hazen 1987). These differences among M_2SiO_4 olivines, chrysoberyl, and $LiScSiO_4$ may be related to differences in the relative compressibilities of the constituent polyhedra. In previous high-pressure studies of olivine structural variations, all authors agreed that the T tetrahedron is the least compressible polyhedron in these materials, with a polyhedral bulk modulus of 300 GPa or greater. The 320 ± 90 GPa value of the present study conforms to the previous work. Compression of this tetrahedron contributes little to the net volume change of the olivine structure, but the short O2-O3 shared edges between T and M1, and the O3-O3 shared edge between T and M2, place constraints on octahedral changes with pressure.

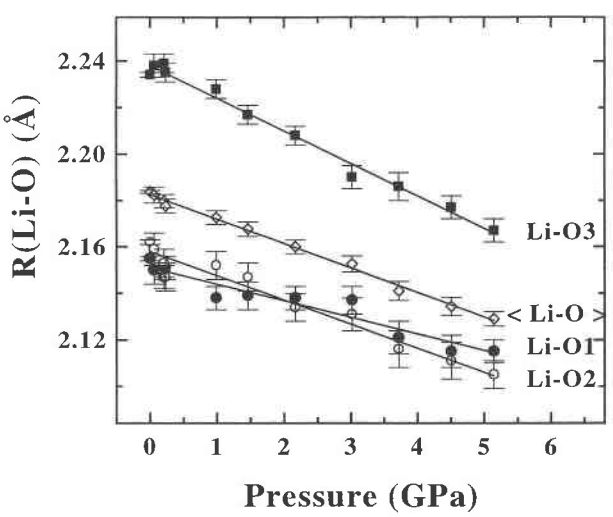

FIGURE 2. Variation of Li-O bond distances with pressure. The longer Li-O3 and Li-O2 bonds are more compressible than the Li-O1 bond.

The relative compressibilities of M1 and M2 vary depending on olivine composition. The Ca-bearing M2 octahedron of monticellite is significantly more compressible than Mg-bearing M1; M2 also appears to be slightly more compressible than M1 in forsterite and fayalite (Kudoh and Takeuchi 1985; Kudoh and Takeda 1986). In the more nearly isotropic chrysoberyl and $LiScSiO_4$, however, M1 is significantly more compressible than M2. It thus appears that the unusual isotropic compression behavior of $LiScSiO_4$ is a consequence of the extreme differences in the compressibility of Li, Sc, and Si polyhedra, in particular the three-times greater compressibility of Li-O bonds in the M1 octahedron in comparison with the compressibility of Sc-O bonds in the M2 octahedron. Li-O bonds in M1 are significantly more compressible than M^{2+}-O bonds, whereas Sc-O bonds in M2 are significantly less compressible than M^{2+}-O bonds. These differences increase *a* compression and decrease *b* compression relative to natural silicate olivines, thus leading to more isotropic behavior.

Polyhedral distortions and interpolyhedral angles

In the previous high-pressure studies of forsterite, monticellite, and chrysoberyl, polyhedral distortions were not observed to change appreciably with pressure. This behavior contrasts with that of the Li octahedron in $LiScSiO_4$, which becomes significantly less distorted with increasing pressure. Compressibilities of the three distinct Li-O bonds, M1-O1, M1-O2, and M1-O3, are 0.0033, 0.0048, and 0.0063 GPa^{-1}, respectively (see Fig. 2). Thus, the longer M1-O2 and M1-O3 bonds are, respectively, approximately 45 and 90% more compressible than M1-O1. These bonds lie close to the *a-b* plane and must therefore contribute to the relative compressibilities of those axes.

Previous high-pressure studies of olivine structural variations also concluded that interpolyhedral angles do not vary significantly with pressure; no significant changes

TABLE 7.—*Continued*

P (GPa)	Li-O2-Sc	Si-O3-Li	Si-O3-Sc	Si-O3-Sc	Li-O3-Sc	Li-O3-Sc	Sc-O3-Sc
0	123.00(6)	87.78(6)	95.18(6)	123.76(7)	94.04(5)	115.49(6)	129.91(7)
0.06	123.0(2)	87.9(2)	95.0(2)	124.4(4)	93.7(2)	115.6(2)	129.6(2)
0.21	123.4(2)	87.9(2)	95.0(2)	124.3(3)	93.7(2)	115.6(2)	129.6(2)
0.23	123.3(2)	87.8(2)	95.1(2)	123.8(3)	93.9(2)	115.6(2)	129.9(2)
0.99	123.4(2)	87.5(2)	95.2(2)	124.0(3)	93.9(2)	115.6(2)	129.8(2)
1.46	123.6(2)	87.9(2)	95.1(2)	124.2(3)	94.0(2)	115.8(2)	129.4(2)
2.17	123.9(2)	87.9(2)	94.9(2)	123.8(3)	94.1(2)	116.2(2)	129.5(2)
3.02	124.0(2)	87.8(2)	95.3(2)	123.0(4)	94.7(2)	116.1(2)	129.6(2)
3.72	124.7(2)	88.0(2)	95.1(3)	123.9(4)	94.3(3)	116.2(2)	129.0(2)
4.51	124.6(2)	87.5(2)	95.2(3)	123.5(4)	94.5(3)	116.3(2)	129.5(2)
5.15	124.9(2)	87.5(2)	95.1(2)	123.5(3)	94.6(2)	116.4(2)	129.3(2)
Int.	123.11(7)	87.85(8)	95.09(5)	124.09(14)	93.81(8)	115.55(4)	129.75(9)
Slope	0.35(3)	−0.05(3)	0.14(2)	−0.13(5)	0.17(3)	0.17(2)	−0.10(3)

are observed in cation-O-cation angles in forsterite, monticellite, or chrysoberyl. In $LiScSiO_4$, however, the Si-O2-Sc angle, which lies in the *a*-*b* plane, decreases significantly from 129.4 to 125.9° between room pressure and 5.15 GPa. This decrease, which is accompanied by shortening of O-O distances between Si and Sc polyhedra, contributes a small additional component of compression, particularly to the *b* axis.

CONCLUSIONS

Olivine has long been recognized as an inherently anisotropic structure. Its extreme compressional anisotropy, for example, provides seismologists with a sensitive technique for analyzing the dynamic behavior of olivine-rich portions of the Earth's mantle. The nearly isotropic compression of $LiScSiO_4$ olivine, therefore, is anomalous. The principal conclusion of this high-pressure structure investigation is that the nearly isotropic compression of $LiScSiO_4$ is, ironically, a consequence of the extremely nonuniform compression of its cation-O bonds. Tetrahedral Si-O and M2 octahedral Sc-O bonds are relatively incompressible, whereas M1 octahedral Li-O bonds are more compressible than any previously recorded in olivines. The vibrational anisotropy of Li in M1 and the significant decrease in distortion of the M1 octahedron with pressure, both features not previous observed in silicate olivines, further contribute to this unexpected behavior.

ACKNOWLEDGMENTS

X-ray diffraction work at the Geophysical Laboratory is supported by NSF grant EAR-9218845 and by the Carnegie Institution of Washington. High-pressure studies are supported in part by the NSF Center for High Pressure Research.

REFERENCES CITED

Becker, P., and Coppens, P. (1974) Extinction within the limit of validity of the Darwin transfer equations: General formalisms for primary and secondary extinction and their application to spherical crystals. Acta Crystallographica, A30, 129–147.

Downs, R.T., Zha, C.-S., Duffy, T.S., and Finger, L.W. (1996) The equation of state of forsterite to 17.2 GPa and effects of pressure media. American Mineralogist, 81, 51–55.

Finger, L.W., and Prince, E. (1975) A system of Fortran IV computer programs for crystal structure computations. National Bureau of Standards Technical Note 854.

Green, H.W., III (1994) Solving the paradox of deep earthquakes. Scientific American, 271(3), 64–71.

Hazen, R.M. (1976) Effects of temperature and pressure on the crystal structure of forsterite. American Mineralogist, 61, 1280–1293.

——— (1977) Effects of temperature and pressure on the crystal structure of ferromagnesian olivine. American Mineralogist, 62, 286–295.

——— (1987) High-pressure crystal chemistry of chrysoberyl, Al_2BeO_4: Insights on the origin of olivine elastic anisotropy. Physics and Chemistry of Minerals, 14, 13–20.

Hazen, R.M., and Finger, L.W. (1979) Bulk modulus-volume relationship for cation-anion polyhedra. Journal of Geophysical Research, 84, 6723–6728.

——— (1980) Crystal structure of forsterite at 40 kbar. Carnegie Institution of Washington Year Book, 79, 364–367.

——— (1982) Comparative crystal chemistry, 231 p. Wiley, New York.

Ibers, J.A., and Hamilton, W.C., Eds. (1974) International tables for X-ray crystallography, vol. IV, 366 p. Kynoch, Birmingham, U.K.

Ita, J., and Stixrude, L. (1992) Petrology, elasticity, and composition of the mantle transition zone. Journal of Geophysical Research, 97, 6849–6866.

Ito, J. (1977) Crystal synthesis of a new olivine, $LiScSiO_4$. American Mineralogist, 62, 356–361.

Kudoh, Y., and Takeda, H. (1986) Single crystal X-ray diffraction study on the bond compressibility of fayalite, Fe_2SiO_4 and rutile, TiO_2 under high pressure. Physica, 139 and 140B, 333–336.

Kudoh, Y., and Takeuchi, Y. (1985) The crystal structure of forsterite Mg_2SiO_4 under high pressure up to 149 kb. Zeitschrift für Kristallographie, 171, 291–302.

Lehmann, M.S., and Larsen, F.K. (1974) A method for location of the peaks in step-scan-measured Bragg reflexions. Acta Crystallographica, A30, 580–584.

Lumpkin, G.R., and Ribbe, P.H. (1983) Composition, order-disorder and lattice parameters of olivines: Relationships in silicate, germanate, beryllate, phosphate and borate olivines. American Mineralogist, 68, 164–176.

Press, W.H., Flannery, B.P., Teukolsky, S.A., and Vetterling, W.T. (1986) Numerical recipes, 818 p. Cambridge University Press, U.K.

Ralph, R., and Finger, L.W. (1982) A computer program for refinement of crystal orientation matrix and lattice constants from diffractometer data with lattice symmetry constraints. Journal of Applied Crystallography, 15, 537–539.

Robinson, K., Gibbs, G.V., and Ribbe, P.H. (1971) Quadratic elongation: A quantitative measure of distortion in coordination polyhedra. Science, 172, 567–570.

Russo, R.M., and Silver, P.G. (1995) The Andes' deep origins. Natural History, 104(2), 52–59.

Sharp, Z.D., Hazen, R.M., and Finger, L.W. (1987) High-pressure crystal chemistry of monticellite, $CaMgSiO_4$. American Mineralogist, 72, 748–755.

Steele, I.M., Pluth, J.J., and Ito, J. (1978) Crystal structure of synthetic $LiScSiO_4$ olivine and comparison with isotypic Mg_2SiO_4. Zeitschrift für Kristallographie, 147, 119–127.

Manuscript received March 30, 1995
Manuscript accepted October 31, 1995